

# EVIDENCE FOR AN EDGE-ON DISK AROUND THE YOUNG STAR MWC 778 FROM INFRARED IMAGING AND POLARIMETRY

MARSHALL D. PERRIN<sup>1</sup>

Division of Astronomy, University of California, Los Angeles, CA 90095  
 mperrin@ucla.edu

WILLIAM D. VACCA

SOFIA-USRA, NASA Ames Research Center, Moffett Field, CA 94035  
 wvacca@sofia.usra.edu

AND

JAMES R. GRAHAM<sup>1</sup>

Dept. of Astronomy, University of California, Berkeley, CA 94720-3411  
 jrg@berkeley.edu

ACCEPTED TO AJ: March 2, 2009

## ABSTRACT

MWC 778 is an unusual and little-studied young stellar object located in the IC 2144 nebula. Recent spectroscopy by Herbig and Vacca (2008) suggested the presence of an edge-on circumstellar disk around it. We present near-infrared adaptive optics imaging polarimetry and mid-infrared imaging which directly confirm the suspected nearly-edge-on disk around MWC 778 ( $i \sim 70^\circ - 80^\circ$ ) plus reveal a more extensive envelope pierced by bipolar outflow cavities. In addition, our mid-infrared images and near-infrared polarization maps detect a spiral-shaped structure surrounding MWC 778, with arms that extend beyond  $6''$  on either side of the star.

Although MWC 778 has previously been classified as an Herbig Ae/Be star, the properties of its central source (including its spectral type) remain fairly uncertain. Herbig & Vacca (2008) suggested an F or G spectral type based on the presence of metallic absorption lines in the optical spectrum, which implies that MWC 778 may belong to the fairly rare class of Intermediate-Mass T Tauri Stars (IMTTs) which are the evolutionary precursors to Herbig Ae/Be objects. Yet its integrated bolometric luminosity,  $\gtrsim 750L_\odot$  (for an assumed distance of 1 kpc) is surprisingly high for an F or G spectral type, even for an IMTT. We speculate on several possible explanations for this discrepancy, including its true distance being much closer than 1 kpc, the presence of a binary companion, and/or a non-stellar origin for the observed absorption lines.

*Subject headings:* stars: individual (MWC 778), stars: pre-main-sequence, circumstellar matter, planetary systems: protoplanetary disks

## 1. INTRODUCTION

Most, if not all, low- and intermediate-mass stars form surrounded by massive disks of gas and dust, which persist for a few million years before dissipating. These disks play important roles in regulating stellar angular momentum, launching bipolar winds and outflows, and, for a substantial fraction of stars, giving rise to planetary systems. Modeling a disk's spectral energy distribution (SED) alone provides only limited insight into these processes because young disks are optically thick, resulting in degeneracies between model parameters and ambiguous interpretations (Chiang et al. 2001). Spatially resolved images in scattered light are generally needed in order to break these degeneracies, and thereby probe the disks' complex structures (Watson et al. 2007).

The two most well-known and well-studied classes of pre-main-sequence (PMS) stars are the T Tauri and Herbig Ae/Be stars. The observational distinction between these two classes is based on spectral type: young stars cooler than F-type are considered T Tauris while hotter ones are called Herbig Ae/Be stars.

Typically, T Tauri stars are interpreted to be PMS stars of roughly solar mass or less, while Herbig Ae/Be stars are young stars of intermediate mass,  $2M_\odot < M < 8M_\odot$ . But such a one-dimensional classification cannot fully represent the range of PMS stellar properties, which depend on both mass and age. This is particularly true for intermediate-mass stars, which are stable against convection and consequently evolve horizontally across the Hertzsprung-Russell diagram towards the main sequence, rising in surface temperature and changing in spectral type as they go. As very young intermediate-mass stars contract toward becoming Herbig Ae/Be stars, they first pass through a stage in which they are classified as T Tauri stars, but ones with vastly higher luminosity than typical. These "intermediate-mass T Tauri stars" (IMTTs; Calvet et al. 2004) are the youngest intermediate-mass stars available for observation at visible or near-IR wavelengths. Due to the slope of the stellar initial mass function and the rapid speed at which stars evolve through this early stage, IMTTs are relatively rare and have been the subject of few detailed studies. Yet these objects potentially offer insights into many aspects of the star formation process, such as the dissipation of stars' natal molecular clouds

<sup>1</sup> Center for Adaptive Optics, University of California, Santa Cruz, CA 95064, U.S.A.

and the properties of circumstellar disks at very young ages.

MWC 778 (= IRAS 05471+2351) is an unusual, and little-studied, object located in the IC 2144 nebula in the direction of the Galactic anticenter. Herbig & Vacca (2008; hereafter HV08) recently presented high resolution optical and moderate resolution near-infrared spectra of MWC 778 and its surrounding nebulosity. These spectra suggest that MWC 778 is a mid- to late-type PMS star with a bolometric luminosity of several hundred  $L_{\odot}$  — in other words, it appears that it may be an IMTTS, though this classification is far from certain, as we will discuss below. Their spectra furthermore imply the presence of a circumstellar disk around MWC 778, inclined close to edge-on to our line of sight.

In this paper, we present near-IR adaptive optics (AO) imaging polarimetry and mid-IR imaging that resolve this disk, confirming the interpretation of HV08. These observations were taken as part of a larger survey of Herbig Ae/Be stars with adaptive optics polarimetry and mid-infrared imaging (Perrin 2006). Near-IR differential polarimetry is an effective technique for resolved imaging of circumstellar material because it allows suppression of the extended and time-variable AO point spread function (PSF) halo. Because atmospheric turbulence does not polarize the PSF halo, while dust-scattered light is strongly polarized, differential polarimetry can separate them to reach the fundamental photon noise limit for detection of faint material (e.g. Kuhn et al. 2001; Apai et al. 2004; Perrin et al. 2008).

The following section §2 summarizes earlier studies of MWC 778 and briefly recaps the results of HV08. In §3, we describe our observations: near-IR imaging polarimetry from Lick Observatory and mid-infrared imaging from Gemini North, and §4 presents the results of these observations. In §5 we discuss the implications of these data for the nature of MWC 778 itself and its surrounding nebula, and in particular consider several competing hypotheses for the spectral type and luminosity of the central illuminating source. §6 summarizes our conclusions.

## 2. PREVIOUS STUDIES OF MWC 778

First identified in the Mount Wilson Catalogue of H $\alpha$ -emitting objects compiled by Merrill & Burwell (1949), MWC 778 was classified as Bpe based on a low-dispersion slit spectrogram (obtained by Minkowski) which revealed strong H and Fe II emission lines. Allen (1974) noted that MWC 778 has a large infrared excess due to dust emission, giving it a very unusual SED that rises nearly linearly in a plot of  $\lambda F_{\lambda}$  vs.  $\lambda$  between 1.65 and 18 microns. This rising infrared SED places MWC 778 firmly within the category of Class I YSOs, with a NIR spectral index  $\alpha \sim 0.4$ . Allen also reported the presence of emission lines of H, Fe II, [Fe II], and [S II] in an optical spectrum of the source, and suggested that it was a pre-main sequence Ae or Be star.

García-Lario et al. (1997) classified MWC 778 (= PDS 204 = GLMP 131) as a YSO based on its near-infrared and IRAS colors. They suggested it was associated with the Galactic H II region BFS50 (= IC 2144), and classified it as a BQ[ ] (which is equivalent to B[e] in a more modern classification system) based on the similarity of its moderate-resolution optical spectrum to

that of HD 51585 and other B[e] stars. This spectrum (shown as Fig. F. 1 in Suárez et al. 2006) exhibits numerous permitted and forbidden emission lines, most of which are attributed to Fe II.

Vieira et al. (2003) obtained *UBVRI* photometry of MWC 778 as well as moderate resolution ( $R=9000$ ) optical spectra centered near H $\alpha$ . Although the optical SED was found to be quite red in general (as might be expected for a source with such a large infrared excess), MWC 778 exhibits a very blue  $U - B$  color ( $U - B = -0.27$ ). The H $\alpha$  line was seen to be double-peaked with unequal strengths in the two peaks. They classified the object as B1? and noted the presence of [O I] and [S II] in emission as well. They associated MWC 778 with the  $^{12}\text{CO}$  ( $J = 1 - 0$ ) emission source in the star-forming region WB711 (Wouterloot & Brand 1989), for which Wouterloot et al. (1993) gave a distance of 1.1 kpc and a far-infrared luminosity  $L_{\text{FIR}} = 400L_{\odot}$  (derived from the IRAS fluxes). They noted that the integrated luminosity resulting from the SED combined with the assumed distance led to a location in the HR diagram for MWC 778 that was “out of the expected position for HAeBe stars”.

Herbig & Vacca (2008; hereafter HV08) recently presented high resolution optical ( $R=48000$ ) and moderate resolution near-infrared ( $R=2000$ ) spectra of MWC 778, as well as a deep image taken through an H $\alpha$  filter. They inferred the presence of a circumstellar disk based on the double peaked nature of many of the emission lines. These authors examined the optical spectrum of Vieira et al. (2003) and questioned the reported B spectral type classification. Their own much-higher-resolution optical spectra reveal the presence of rotationally broadened absorption lines from species like Ca I and Fe I, which they claimed were photospheric in origin and based on which they suggested a spectral type for MWC 778 between late A and G. The NIR spectrum exhibits a large number of Fe II and [Fe II] lines as well as the Br series (up to Br 26) and the Pa series (up to Pa 23) in emission. Herbig & Vacca derived an extinction  $A_V \sim 2 - 3$  from a variety of indicators and estimated a distance of  $\sim 1$  kpc based on associations with other star forming regions in the area, but stressed that this value is highly uncertain. Integrating the observed SED using that distance leads to a bolometric luminosity of  $\sim 510L_{\odot}$ . The H $\alpha$  image shown by HV08 looks very similar to the lobed nebula surrounding other B[e] stars (Marston & McCollum 2008). HV08 refer to IC 2144 as a reflection nebula, not an emission nebula (i.e., H II region), though it has also been classified as an H II region by others (e.g. Blitz, Fich & Stark 1982).

## 3. OBSERVATIONS AND DATA REDUCTION

### 3.1. Near-Infrared Imaging Polarimetry

We obtained  $J$ ,  $H$  and  $K_s$  band differential imaging linear polarimetry of MWC 778 with the 3-m Shane telescope at Lick Observatory, using the laser guide star adaptive optics (LGS AO) facility (Gavel et al. 2003) and the IRCAL camera (Lloyd et al. 2000).

A detailed description of the IRCAL polarimeter, the observing procedures, and the associated data reduction pipeline can be found in Perrin et al. (2008). Briefly, a Wollaston prism within IRCAL forms simultaneous images of perpendicular polarizations on the detector,

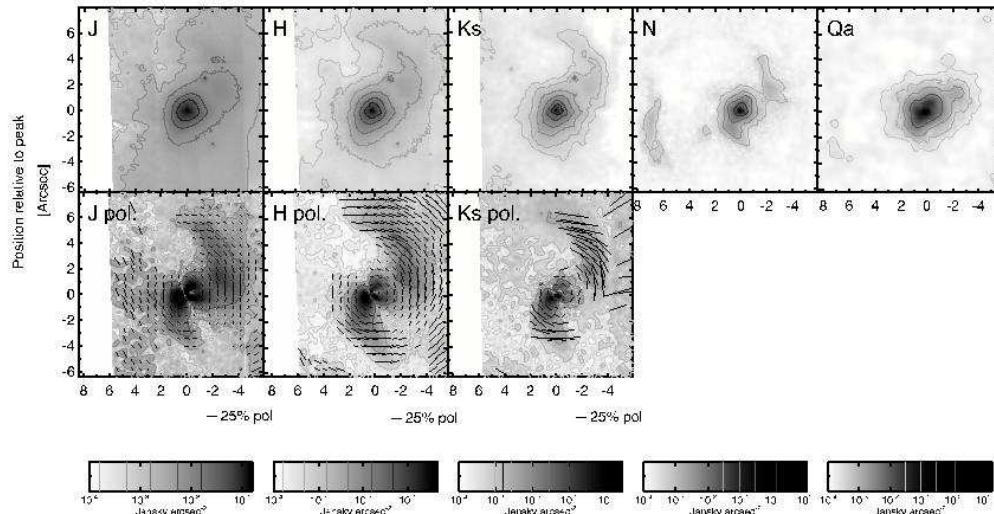


FIG. 1.— **Top row:** Total intensity near- and mid-infrared images of MWC 778. The display scales for each wavelength are shown below, with contour levels as indicated. **Bottom row:** Polarized intensity images in *J*, *H*, and *K* bands, with vectors showing polarization fraction and orientation. The display scales for polarized intensity are reduced 100x relative to the scales for total intensity shown in the scale bars. North is at the top, east to the left in all images. Immediately around MWC 778, the near-IR polarization maps reveal two bright lobes bisected by a narrow dark lane with a position angle of  $\sim 25^\circ$  (See also Figure 2 for a closer view). This region is embedded in a larger spiral-shaped nebula, which can be seen extending to at least  $6''$  radius on either side of the star. It is particularly visible in the *N'* image, where the northwest spiral arm can be seen to wrap  $180^\circ$  around the star.

and a rotating half-wave plate modulates the observed polarization state while a sequence of images are taken. After bias and flat-field correction, the images for each linear polarization (corresponding to a given waveplate rotation) are mosaiced together. The sums and differences of the resulting mosaic images then give the Stokes *I*, *Q* and *U* parameters describing linear polarization. To improve sensitivity to faint signals, the reduced images presented in this paper were adaptively smoothed by convolution with a 3-resolution-element wide Gaussian in regions with signal to noise (*S/N*) < 1 per pixel, decreasing to one resolution element wide for  $1 < S/N < 10$ , and no smoothing for pixels with *S/N* > 10. The near-IR total intensity images are shown in Figure 1 (top row), along with the linear polarized intensities  $P = (Q^2 + U^2)^{1/2}$ , where *Q* and *U* are the usual Stokes parameters.

These observations were taken on 2005 Nov 23, during a period of unseasonably warm weather and good seeing: Fried’s parameter  $r_0$  was 15-20 cm that night. For MWC 778, our total exposure times in *J*, *H*, and *K<sub>s</sub>* bands were 720 s, 640 s, and 390 s, respectively. The achieved point spread function (PSF) full width at half maximum (FWHM) was  $0.29''$  at *J*,  $0.21''$  at *H*, and  $0.20''$  at *K<sub>s</sub>*, as measured from the star  $2.8''$  northwest of MWC 778. Because MWC 778 itself is resolved, we cannot measure PSF Strehl ratios directly on it, and the nearby star to the northwest is also unsuitable due to the spatially-variable bright nebosity behind it. As a

proxy, we measured<sup>2</sup> the Strehl ratio for an unresolved star of comparable brightness observed with LGS AO immediately after MWC 778 (PDS 211, *V*=13.7), and found Strehl ratios of  $0.02 \pm 0.01$ ,  $0.07 \pm 0.02$  and  $0.16 \pm 0.03$  for *J*, *H* and *K<sub>s</sub>* respectively, corresponding to 400-500 nm rms wavefront error. For photometric calibration we observed the standard S852-C (Persson et al. 1998) shortly after MWC 778.

Our images reveal a bright point source surrounded by fainter extended nebosity filling most of our  $12'' \times 20''$  field of view (see §4). We performed aperture photometry around MWC 778 using both  $1''$  and  $6''$  radius apertures to estimate the flux from the central bright region alone and the whole observed nebula, respectively (Table 1). There were intermittent cirrus clouds that night, but we observed MWC 778 during a clear period, and our derived photometry is in excellent agreement with that of HV08 taken one month earlier, suggesting that the cirrus did not adversely impact these data. We caution that even the  $6''$  radius does not include the *entire* nebula, only the portion visible within our  $12''$ -wide field of view. In the 2MASS Atlas images, the nebula around MWC 778 is seen to extend at least  $20''$  from the star, and in deeper images would likely appear comparable in size to the *H $\alpha$*  nebula shown in HV08,  $\sim 2$  arcmin across.

<sup>2</sup> Using the `lickstrehl` IDL tool; [http://mthamilton.ucolick.org/techdocs/instruments/ircal/ircal\\_lickstrehl.html](http://mthamilton.ucolick.org/techdocs/instruments/ircal/ircal_lickstrehl.html). See Roberts et al. (2004) for a discussion of the difficulty in measuring Strehl ratios accurately for undersampled instruments such as IRCAL. The algorithm in `lickstrehl` incorporates the best practices identified by Roberts et al., but we caution there may still be systematics particularly at these low correction levels.

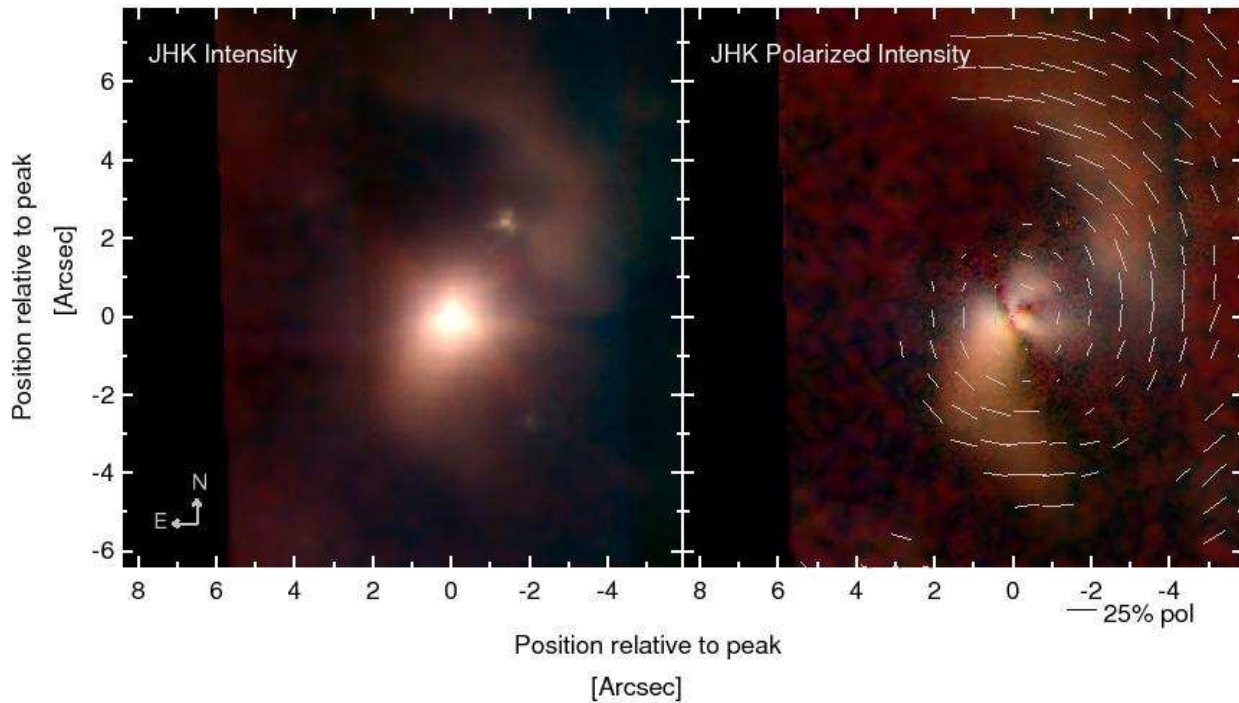


FIG. 2.— IRCAL 3-color near-infrared image of the total intensity and polarization in MWC 778. The overplotted vectors show the polarization position angle and fraction as measured in  $H$  band. The observed dark lane is the characteristic signature of a nearly edge-on circumstellar disk, while the partially-divided northwest nebulosity suggests the limb-brightened edges of a conical cavity in a circumstellar envelope, cleared by bipolar outflows. The location of peak brightness in total intensity (at left) is displaced from the center of the polarization vectors by  $0.15''$ , and at right corresponds in location to the bright region immediately east of the dark lane's middle. This displacement indicates that we do not see the star directly at these wavelengths, but rather observe it entirely in light scattered around the circumstellar disk (See §4.1)

### 3.2. Mid-infrared Imaging

Mid-infrared images of MWC 778 at 11.2 and 18.1 microns ( $N'$  and  $Qa$  bands) were obtained at Gemini North on 2005 Dec 16 using the Mid-Infrared Imager/Echelle Spectrometer (Michelle) instrument (Glasse et al. 1997) as part of program GN-2005B-C-4. The total on-source integration times were 235 s and 218 s, respectively. The chop throw was  $15''$  at a position angle of  $30^\circ$ . Conditions were clear, with good seeing and 2.4 mm of precipitable water vapor.

These data were reduced using custom IDL code that incorporates and extends IDL reduction routines provided by R. S. Fisher at Gemini. A detailed description of this reduction code can be found in Perrin (2006). To remove the thermal background emission, each chop-nod set was reduced using the standard double subtraction method. No flat fielding was done. All chop-nod-subtracted images were registered via Fourier cross-correlation and co-added to generate a final mosaic. The data were then corrected for atmospheric transmission and flux-calibrated via observations of standard stars taken from (Cohen et al. 1999) obtained throughout the night.

The final images have PSF FWHMs of  $0.39''$  at  $N'$  and  $0.54''$  at  $Qa$ , as measured on a calibration star observed immediately after MWC 778. The field of view is  $32'' \times 24''$ . To improve sensitivity to faint signals, these

images were adaptively smoothed by convolution with a 3-resolution-element wide Gaussian in regions with  $S/N < 1$  per pixel, decreasing to one resolution element wide for  $1 < S/N < 10$ , and no smoothing for pixels with  $S/N > 10$ . Photometry was performed on the unsmoothed data, using for consistency the same  $1''$  and  $6''$  apertures as were used for the near-IR data. (See Table 1). We note that the emission observed in  $N'$  actually extends beyond the  $6''$  aperture, primarily in the form of an arc of emission east of MWC 778 just outside the aperture. There is approximately 0.3 Jy of emission from that region in  $N'$ . Along the chopping position angle of  $30^\circ$ , no mid-IR nebulosity is visible beyond  $\sim 7''$  radius at our sensitivity, so the  $15''$  chop throw does not result in any self-subtraction of the nebula.

## 4. THE COMPLEX ENVIRONMENT OF MWC 778

### 4.1. A spatially-resolved, nearly-edge-on disk and bipolar envelope

Immediately around MWC 778, the near-IR polarization maps reveal two bright lobes bisected by a narrow dark lane with a position angle of  $\sim 25^\circ$ . The dark lane is slightly curved, with the concave side facing northwest. On that side, the bright northwest nebulosity further splits into two fans of light separated by a region of lower polarization. The polarization vectors are centrosymmetric throughout, indicating that the

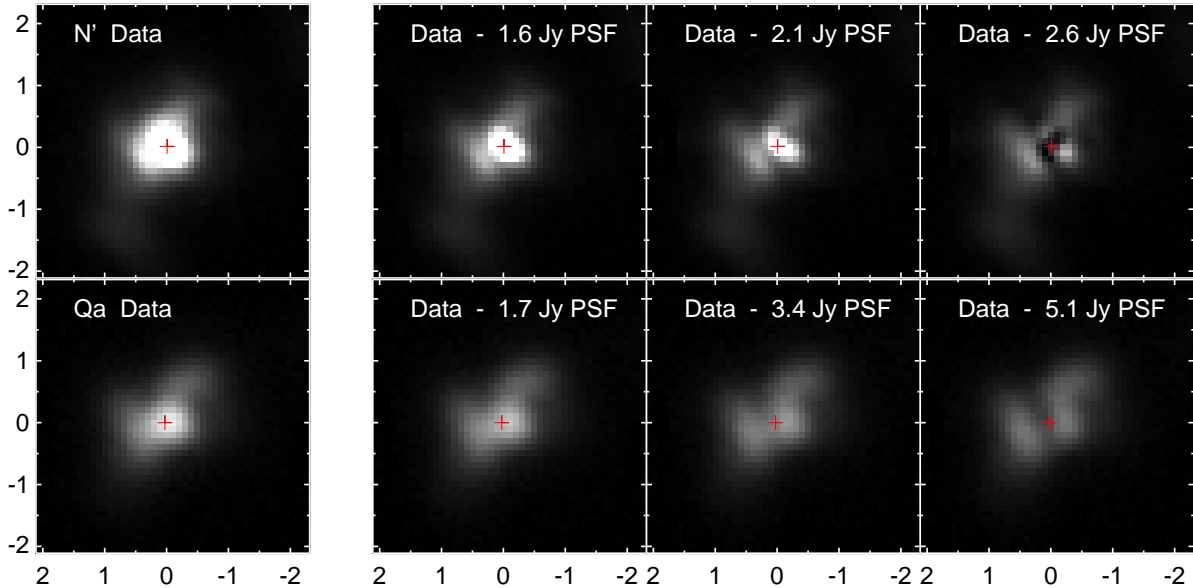


FIG. 3.— Mid-infrared PSF subtractions, showing a mid-IR counterpart to the dark lane seen in the near-IR. The unsubtracted observations are shown at left, while the right panels show PSF subtractions with various flux scalings for the unresolved component. The cross symbols mark the central peak location of the subtracted PSFs. For each wavelength, all four images are shown with the same linear display scaling. The optimal PSF fluxes, 2.1 Jy for  $N'$  and 3.4 Jy for  $Qa$ , were determined empirically based on interactive adjustment of the subtractions to eliminate the central point source and produce smooth residuals; there is considerably uncertainty in their values. Yet the detection of the dark lane is a robust feature of these data, persisting even if the subtracted PSF varies in intensity by  $\pm 25\%$  at  $N'$  or  $50\%$  at  $Qa$ , as shown in the adjacent panels. The mid-IR dark lane appears at the same position angle and with comparable spatial extent to the near-IR dark lane shown in Figure 2, and the midpoint of the mid-IR dark lane is likewise offset  $\sim 0.2''$  southeast of the location of peak flux. The asymmetric nebula on either side of the dark lane also shows a similar bipolar structure consistent with the near-IR.

observed structure is a reflection nebula illuminated by MWC 778. This region is embedded in a larger spiral-shaped nebula, which we discuss below; here we concentrate on the central portion.

The observed dark lane is the characteristic signature of a nearly edge-on circumstellar disk, while the partially-divided northwest nebulosity suggests the limb-brightened edges of a conical cavity in a circumstellar envelope, cleared by bipolar outflows. Overall, MWC 778 bears a striking resemblance to several other young stars known to have nearly-edge-on disks and envelopes with bipolar cavities, for instance LkH $\alpha$  233 (Perrin et al. 2004a). Based in part on discrepancies between optical spectra of MWC 778 and the nearby nebulosity, HV08 inferred the presence of an inclined disk around the star, with its rotational axis pointing to the northwest. We confirm here that suggestion via direct detection of the disk in our polarization maps. The observed rotational axis of the disk agrees with that suggested by HV08.

The position of peak intensity in the total intensity images is shifted about  $0.2''$  (1 resolution element) northwest from the center of the dark lane. This displacement toward the northwest indicates that side of the disk is tipped slightly toward us. The slight curvature of the central dark lane confirms this interpretation: MWC 778's disk is nearly edge-on, but not perfectly so, or it would obscure the central star entirely and the dark lane would be straight. The precise amount of inclination consistent with the observations depends on the disk's structure, such as the amount of flaring, which we currently cannot constrain. However, it seems

probable that the disk is inclined roughly  $70\text{--}80^\circ$  to our line of sight, such that the star is just barely visible around the obscuring disk. The central intensity peak is significantly polarized,  $1.8\% \pm 0.4\%$  at  $H$ , which suggests that in fact we see the star in light scattered around the disk's edge rather than directly.

The apparent polarization fraction rises both at longer wavelengths and with increasing distance from the star. For instance, in the bright part of the southeastern nebula, about  $1.5''$  from the star, the  $J, H, Ks$  polarization fractions are  $\sim 13\%, 16\%,$  and  $18\%$  respectively, while in the curved region  $4''$  northwest of the star, the polarization fractions are  $22\%, 28\%$  and  $34\%$ . However, within the central arcsecond on both sides of the dark lane, the polarization fraction stays approximately constant with wavelength at  $\sim 9\%$ . At face value, this may suggest different dust grain properties closer to the star, as would be expected from collisional aggregation of larger particles. But it is hard to accurately measure polarization fractions with AO data, given the contamination from uncorrected stellar light in the AO PSF halo, so these numbers should be considered cautiously.

Both our mid-IR images show a bright point source at the location of MWC 778, surrounded by extended nebulosity aligned approximately southeast to northwest. In the  $Qa$  image, a hint of the dark lane can be seen, but it is partially obscured by the bright central point source. We therefore subtracted the central source using scaled copies of a PSF reference star observed immediately after MWC 778 (Figure 3). The PSF was aligned with



TABLE 1  
PHOTOMETRY OF MWC 778

Band	Wavelength	$R \leq 1''$ (mag.)	Uncert. (mag.)	$R \leq 1''$ (Jy.)	Uncert. (Jy.)	$R \leq 6''$ (mag.)	Uncert.	$R \leq 6''$ (Jy.)	Uncert.
$J$	1.20	10.37	0.06	0.111	0.006	10.15	0.06	0.136	0.007
$H$	1.60	9.31	0.05	0.197	0.010	9.12	0.05	0.235	0.012
$K_s$	2.05	8.25	0.05	0.323	0.016	8.04	0.05	0.392	0.020
$N'$	11.20	2.27	0.03	3.68	0.076	1.93	0.03	5.08	0.12
$Qa$	18.10	-0.50	0.03	18.56	0.55	-0.91	0.03	27.20	0.60

NOTE. — Photometry of MWC 778, in both  $1''$  and  $6''$  apertures. The measurements are presented as both magnitudes and fluxes. The stated uncertainties include both statistical error and systematic flux calibration uncertainty, conservatively estimated at 5% in the near-IR and 1.5% in the mid-IR. (The more stable mid-IR PSF allows more precise absolute calibration compared to the near-IR AO PSF.) Note that the smaller  $1''$  aperture still contains some amount of resolved nebular flux in addition to the central point source.

the position of the central peak as measured by fitting 2D Gaussians to both, and the overall flux scaling was iteratively adjusted to remove the central peak without oversubtracting the surrounding nebulosity. The optimal flux scalings found this way are not particularly precise (and in fact are somewhat subjective), but the basic result holds true for a wide range of PSF scalings, as shown in Figure 3: Subtracting the central PSF reveals a dark lane in both the  $N'$  and  $Qa$  images, with the same orientation and scale as that seen in the near-IR. The optical depth in the disk midplane must be sufficient to cause appreciable extinction even at  $18 \mu\text{m}$ , implying  $A_V > 50 \text{ mag.}$  in visible light in the disk midplane. The light we see at short wavelengths must scatter out around the disk through paths of much lower extinction.

We caution that the point-source fluxes found in this manner, 2.1 Jy for  $N'$  and 3.4 Jy for  $Qa$ , almost certainly do not represent the photospheric intensity of the central star. Thermal emission from a circumstellar disk on scales of  $\lesssim 100 \text{ AU}$  would be unresolved by these observations. The observed flux levels are far in excess of the expected photospheric flux of any plausible central star, leading us to conclude that in these point sources we are most likely observing thermal emission from the hot inner disk.

The dark lane extends outward for  $\sim 1.2''$  on either side of the star in the near-IR, and almost as far in the mid-IR, corresponding to a physical radius of  $\sim 1200 \text{ AU}$  for an assumed distance of 1 kpc. This is similar in size to other spatially-resolved disks around Herbig Ae/Be stars (e.g. 800 AU for HD 141569, Clampin et al. 2003; 1000 AU for LkH $\alpha$  233, Perrin et al. 2004a; 1100 AU for MWC 480, Simon et al. 2000). The thickness of the dark lane increases with radius from the star: in the near-IR close to the center, the apparent thickness is  $\sim 0.2''$  (about 1 resolution element), but at a radius of  $0.7''$  the thickness has increased to  $0.5\text{--}0.6''$ .

Does the observed extent of the dark lane correspond to the physical diameter of the disk, or are we instead seeing a large shadow cast by a much smaller disk? In their detailed study of disk shadows, Pontoppidan et al. (2005) wrote that the “most important difference between dark lanes due to extinction from a large disk and the dark lanes due to projection is that the former are expected to be entirely dark while the latter will still have a bright source in the center of the system... [For a disk shadow falling on a screen] a dark band should be seen but with a central near-infrared compact source in the center. The presented model never produces a

disk shadow without the central source being at least as bright as the reflecting material.” In the case of MWC 778, no bright point source is visible *within* the dark lane at any wavelength. Instead the bright PSF peak is offset northwest outside of the dark lane at all wavelengths, consistent with light scattering around the edge of an optically thick disk. Hence we conclude that the observed morphology is primarily due to a physically large disk with apparent angular radius  $\sim 1''$ , rather than shadowing from a much smaller disk.

#### 4.2. A giant spiral?

On larger scales the polarized intensity maps and mid-infrared images exhibit a pair of curving “spiral arms” that wrap counterclockwise around the central disk. This is an infrared counterpart to the “reverse question mark”-shaped dark lane HV08 saw<sup>3</sup> in their H $\alpha$  image; the spiral arms we see in the near- and mid-infrared are coincident with the bright outline of the “question mark”, while the darker region inwards of the spiral forms the “question mark” itself. Although this overall structure can be discerned in total intensity images, particularly in our  $K_s$  and  $N'$  images and the H $\alpha$  image of HV08, it is especially prominent in our linear polarization maps (Figure 1).

The spiral is asymmetric: the southeastern arm is both shorter and more tightly curved than the northwestern arm. It appears to have a distinct corner about  $3.5''$  southwest of the star, a sharp feature also clearly seen in the  $N'$  image. The southeast arm trails off about  $6''$  from the star at PA= $195^\circ$ , while the opposite northwest arm fades out in our near-IR images around  $r = 7''$ , PA= $15^\circ$ . That places its apparent termination almost exactly  $180^\circ$  opposite the end of the southern arm, though a bit more distant from the star.

Our mid-infrared images and the H $\alpha$  images of HV08 (see their Fig. 3) show that this “northwestern” spiral arm in fact continues onward to wrap nearly  $180^\circ$  around the source, albeit at reduced brightness for much of that arc. It becomes brighter again in a region  $\sim 6''$  to the E of MWC 778, seen prominently in the H $\alpha$ ,  $N'$ , and  $Qa$  images. This bright region is mostly outside the field of

<sup>3</sup> We note that another spiral structure can also be seen on a vastly larger scale in HV08’s H $\alpha$  image (see their Fig. 1). This image reveals a faint, diffuse, “spiral” feature beginning almost due west (PA= $270^\circ$ ) of MWC 778 and extending nearly an arcminute from MWC 778 while wrapping  $90^\circ$  around the source to end at PA= $0^\circ$ . It is not clear if there is any connection between the two spiral features.

view of our near-IR images, but can partially be seen at the extreme southeast corner of the polarized intensity maps. Curiously, near the base of the northwestern arm a partial gap can be seen, a region of reduced polarized intensity between  $1.5 - 2.4''$  from the star. No similar gap is seen in the southeastern arm.

We discuss possible explanations for this spiral structure in §5.2 below.

#### 4.3. Detection of Candidate Companion Stars

HV08 noted that if MWC 778 is indeed a massive YSO, then we should expect it to be surrounded by a cluster of lower-mass YSOs. In our AO data, two fainter stars are visible near MWC 778; see Figure 2, where these point sources are apparent at roughly  $(-2'', -2'')$  and  $(-1.5'', 2'')$  from MWC 778. Table 2 presents the photometry and astrometry of these potential companions. Neither of these stars are visible in our mid-IR data. It remains unknown whether these are physically associated young stars or merely foreground objects. Given the amount of circumstellar dust around MWC 778, it seems unlikely for them to be background objects.

In addition, in our  $N'$  image, two other faint point sources ( $\Delta N' \sim 7$  mag.) are detected several arcseconds southwest of MWC 778. Both of these objects fall outside the field of view of our near-IR data (and consequently are not shown in Figure 1, where we have cropped the mid-IR images to the same FOV as the near-IR data). However, their positions match known point sources from the 2MASS catalog. These two sources are also included in Table 2.

On the other hand, the 2MASS “point sources” 2MASS 05501321+2352179, 05501322+2352242, 05501418+2352115, 05501438+2352132, and 05501443+2352175 correspond to the resolved nebulosity around MWC 778. We see no evidence in our data of actual point sources at those locations.

### 5. DISCUSSION

HV08 presented optical spectra that showed MWC 778 and its nearby nebulosity differ strikingly in which emission lines are present and in the shapes and velocities of those lines. They suggested that these spectral discrepancies could be explained if the star was seen through a rotating edge-on disk, while the portion of the nebula they observed (northwest of MWC 778) was directly illuminated by the star through a polar cavity perpendicular to the disk plane. Our observations resolve the disk and bipolar envelope with precisely the orientation claimed by HV08, and confirm their interpretation is correct.

But many other questions still remain open about MWC 778. One of the most fundamental questions is the distance, which remains very uncertain. The value of 1 kpc adopted by HV08 was based on distances to a handful of other clouds and star forming regions in that part of the sky, ranging from 0.4 to 2 kpc, despite the fact that MWC 778 is not known to be physically associated with any of those clouds. This uncertainty in the distance to MWC 778 impacts our ability to assess its physical properties and evolutionary state.

#### 5.1. IC 2144 is a Reflection Nebula

IC 2144, the nebula around MWC 778, has previously been described as both a reflection and an emission nebula (see §2). HV08 considered IC 2144 to be a reflection nebula, but did not explicitly state their reasoning behind this classification. Three factors contributed to their classification (G. Herbig, private communication 2008): 1. None of their high-resolution optical spectra show any signs of the [O III]  $\lambda\lambda 4959, 5007$  emission lines, which are ubiquitously found in H II regions. 2. The  $H\alpha$  emission line seen from the nebula has FWHM  $\sim 3 \text{ \AA}$ , as broad as the  $H\alpha$  emission from MWC 778 itself, and in contrast to the generally narrow emission typically seen from H II regions (FWHM  $\sim 0.5 \text{ \AA}$ ). 3. The spectrum of MWC 778 itself shows absorption lines indicative of a relatively cool spectral type (e.g. Li I, Ca I, Fe I), and lacks any absorption lines (e.g. He I and N III) that would indicate the presence of an OB star capable of photoionizing the nebula. An additional piece of circumstantial evidence against IC 2144 being an emission nebula is that it was not detected in a VLA survey of candidate H II regions at 5 GHz by Fich (1993), implying an upper limit to free-free emission from ionized gas of  $< 3 \text{ mJy}$ , versus  $50\text{--}10^4 \text{ mJy}$  for typical H II regions detected in that survey. Together these facts provide strong evidence that the optical nebula is seen in reflected starlight.

The centrosymmetric polarization pattern we observe now establishes unambiguously that IC 2144 is primarily a reflection nebula illuminated by MWC 778. Our measurement directly confirms this at near-infrared wavelengths, and in combination with the spectral information from HV08 (particularly the lack of [O III] emission and the width of the  $H\alpha$  line) we conclude that the optical nebula almost certainly has its origins in reflection as well. It would be straightforward to confirm this through optical imaging polarimetry of IC 2144, or flux-calibrated narrow-band imaging in  $H\alpha$  and an adjacent continuum filter.

The mechanism creating the extended mid-infrared light is less clear. Scattered light may still be a significant, perhaps dominant, effect, but we cannot rule out contributions by thermal emission from transiently heated dust grains or fluorescent emission from polycyclic aromatic hydrocarbons. Mid-IR spectroscopy of the extended nebula would allow the nature of the emission there to be determined.

#### 5.2. What is the nature of the central source?

Based on its spectrum showing many emission lines indicative of accretion plus absorption from lithium (HV08), the presence of extensive surrounding nebulosity, and the fact that its SED is still rising past 60 microns, MWC 778 appears to be a young star. We can attempt to determine its nature more precisely by inferring its position along pre-main-sequence evolutionary tracks based on its observed properties, but the large uncertainty in its distance prevents us from unambiguously placing MWC 778 on such tracks.

Using their estimated 1 kpc distance, HV08 integrated MWC 778’s SED to obtain a bolometric luminosity of  $\sim 510 L_{\odot}$ , in agreement with previous estimates (see §2). However, the presence of the disk implies that the source suffers more extinction than was assumed by HV08. In fact the total extinction around the star must depend on

TABLE 2  
NEARBY SOURCES

Source	$\rho$	$\theta$	$\Delta J$	$\Delta H$	$\Delta K_s$	$\Delta N'$
MWC 778 NIR1	2.81	330.6	4.22	4.27	4.83	-
MWC 778 NIR2	3.29	216.9	5.65	6.24	6.99	-
2MASS 05501333+2352136	8.95	239.4	-	-	-	7.32
2MASS 05501303+2352140	13.08	253.5	-	-	-	7.09

NOTE. — Properties of other sources detected in our fields of view. The two near-IR sources were not detected in the mid-IR data, while the  $N'$  point sources are outside the field of view of our near-IR data. Astrometry is relative to MWC 778, and photometry at each wavelength is relative to the observed flux of MWC 778 measured within a  $1''$  aperture, though the photometry of these stars used  $0.5''$  apertures to reduce contamination from the nebula. Aperture corrections were applied based on subsequent observations of photometric standard stars. Derived uncertainties are  $\Delta\rho = \pm 0.05''$ ,  $\Delta\theta = 1^\circ$ , and  $\sim 5\%$  for the relative photometry. The near-IR point sources are both visible near MWC 778 in Figure 2. The mid IR point sources are not shown in any of the figures here due to the field of view selected for display.

the line of sight, from hundreds of magnitudes directly through the disk midplane to only a few magnitudes or less for light scattering out along the polar cavities. (Thus our statement in §4.1 of  $A_V > 50$  in the midplane is not incompatible with HV08's estimated  $A_V \sim 3$  in total integrated light, since the latter was derived from the relative strengths of emission lines seen in light that presumably traveled through low extinction regions.) Whitney et al. (2003) computed model SEDs for class I YSOs surrounded by disks plus bipolar envelopes (like MWC 778), and found that over a wide range of inclinations the true bolometric luminosity was typically  $1.5 - 2\times$  the observed luminosity. If we correct for MWC 778's non-isotropic radiation using this factor, its bolometric luminosity increases to  $750L_\odot$  or more. Because the total amount of extinction is uncertain, this should be taken as a lower limit: Luminosity correction factors of  $10\times$  or higher have been derived for other disk+bipolar envelope systems (e.g. Perrin et al. 2007), so it seems possible that MWC 778's luminosity could be as high as several thousand  $L_\odot$ .

When combined with the F-G spectral type claimed by HV08, a luminosity of  $\geq 750 L_\odot$  presents a conundrum, as it is far larger than that of any other known IMTTS. That luminosity, along with an effective temperature of  $\sim 7000$  K (for an F star), would place MWC 778 well above the birthline in the HR diagram expected for any intermediate mass stars (Palla & Stahler 1990; Palla 2005). Although the exact position of this stellar birthline varies depending on the protostellar mass accretion rate, there is no evidence that such rates are ever high enough to allow for a  $750 L_\odot$  F star; the birthline appears to be a firm boundary on allowable stellar parameters (Palla 2005). We thus must reject the notion that MWC 778 could really be a single F or G star with  $L \geq 750 L_\odot$ .

A similar conclusion can be reached if we use the calibrations between Br  $\gamma$  and Pa  $\beta$  luminosities and accretion luminosity given by Calvet et al. (2000, 2004). The observed line luminosities of MWC 778 from HV08 yield a lower limit to the accretion luminosity of  $\sim 12L_\odot$ . This is several times larger than accretion luminosities measured for even the most luminous objects in the Calvet et al. (2004) sample of IMTTS, again indicating an alternate explanation for MWC 778 must be sought.

The high total and accretion luminosities could instead be consistent with MWC 778 being a Herbig Be star around  $\sim 5 M_\odot$ . Indeed, most claimed spectral types

for MWC 778 prior to HV08 were of type B (B1?e, Vieira et al. 2003; BQ[ ], Suárez et al. 2006), and similar emission-line-dominated spectra are seen for Be stars such as LkHa 101 or MWC 1080. In HV08's data, MWC 778 does not show any absorption lines such as He I which would indicate the presence of an OB star (though emission features could potentially hide such lines). The fact that IC 2144 is a reflection nebula, not a photoionized HII region, places an upper limit on the amount of ionizing flux which could be present, inconsistent with spectral types hotter than B1, but we cannot rule out a mid-B star on this basis. Nevertheless, HV08 unambiguously detected optical absorption lines such as Ca I 6102.72 Å, Fe I 6136.63/6137.70 and Li 6707 Å, which require cooler temperatures consistent with F-G spectral type and inconsistent with classification as a Be. The  $v \sin i$  of those features is  $\sim 30 \text{ km s}^{-1}$ , a typical value for an F5 star but much less than would be expected for any B or A star seen at high inclination ( $v \sin i > 100 - 200 \text{ km s}^{-1}$ ). The observed features are shallow, suggesting veiling, but their detection is clear and any model of MWC 778 must account for them.

There are (at least) three possible explanations for the apparent discrepancy between MWC 778's large bolometric luminosity and the presence of metallic absorption lines that suggest a late spectral type: (1) The first and simplest explanation is that the distance is not 1 kpc, hence the luminosity is wrong; (2) alternately, the absorption lines reported by HV08 may arise from the atmosphere of the accretion disk, rather than the stellar photosphere, hence the spectral type is wrong; (3) the source may be a binary system consisting of a B-type star and an F-type star. We now consider each of these in turn.

If we invoke a smaller distance, how close could it plausibly be? A potential lower limit comes from the fact that based on projected stellar densities, IC 2144 appears to be more distant than the cloud containing RR Tau at 380 pc (see HV08 §1). If the distance to MWC 778 is actually 500 pc, rather than 1 kpc, the luminosity decreases to  $180 L_\odot$  (and the disk radius would decrease to about 600 AU). The observed absorption line depths are shallow, consistent with additional continuum veiling  $\sim 3\times$  greater than the intrinsic stellar photosphere (see Figure 7 in HV08). This would reduce the actual stellar luminosity to about  $45 L_\odot$ , approximately in line with that expected for a F-type IMTTS or a Herbig Ae star near the birth line.



But a non-stellar origin for the absorption spectra may offer an equally plausible means of reconciling the observed luminosity and spectrum. If MWC 778 is an early to mid-type Be star, surrounded by a protoplanetary disk with a nearly edge-on inclination, light reaching us must propagate nearly parallel to the disk's surface, and indeed must scatter from dust in the optically thin surface layers to produce the observed polarization. Since this propagation path passes through gas as well as dust, the former will produce absorption lines in the spectra. To impose F/G type absorption lines on an originally near-featureless Be star spectrum requires gas temperatures of several thousand degrees, several times larger than the expected dust destruction temperature. However, Kamp & Dullemond (2004) showed that the gas and dust temperatures decouple in a protoplanetary disk's upper atmosphere, and that the gas between the dust disk's surface and a few AU above the disk can be as hot as  $10^4$  K at distances of tens of AU from a T Tauri star. A similar disk atmosphere model would need to be calculated for a Be star to investigate whether a sufficient optical depth of gas at 6000–7000 K could be available in the disk atmosphere of MWC 778 to produce the observed lines. In this scenario, the 30  $\text{km}^{-1}$  widths of the absorption lines would be due to the superposition of light scattered toward us from multiple portions of the rotating disk, each with its own Keplerian velocity relative to us.

Finally, it is possible that MWC 778 is a binary system, consisting of a B star and an F star, similar to Z CMa (e.g., Whitney et al. 1993). The high resolution optical spectra obtained by HV08 reveal no evidence of velocity shifts in the absorption lines due to orbital motions, but the signal-to-noise ratio of these features is low, and the upper limit on any velocity shifts is large ( $< 10$  km/s; Herbig, private communication). To investigate how detectable binarity would be given HV08's two spectroscopic observations separated by about one year, we performed Monte Carlo simulations of binary systems with a  $4M_{\odot}$  primary and an inclination of 70 deg, for companion masses ranging from the substellar mass limit to  $4M_{\odot}$ , under the assumption that the observed absorption lines arise in the atmosphere of the lower-mass component. These simulations indicate that the observations of HV08 would have detected line shifts of  $\geq 10 \text{ km s}^{-1}$  with a probability of  $\sim 0.9$  if there existed any companion with a semi-major axis  $a < 5$  AU, roughly independent of companion mass. Therefore we can rule out such a close binary in MWC 778. However, the existing observations have only a probability of  $\sim 0.5$  of detecting any binary companion with  $5 < a < 10$  AU, and are completely insensitive to binaries with larger semi-major axes  $a > 10$  AU.

Examination of the evolutionary tracks by Palla & Stahler (1990) indicate that a binary system consisting of a late B star and an early F star in which both stars sit on the birth line could just produce the estimated luminosity for MWC 778. Such a system would have approximately the correct secondary-to-primary flux ratio ( $\sim 0.2$ , based on HV08's observation that the F-type metal absorption lines are about a factor of 3-4 weaker than expected from a normal F star). However this is the largest luminosity such a binary could have; as soon as the stars age and move off the birth line, the total luminosity drops

precipitously. For an age of 1 Myr, such a system would be expected to have a total luminosity of only  $\sim 170L_{\odot}$ . In short, a B star + F star binary system could explain the observed properties of MWC 778 only if either the system is extremely young ( $< 1$  Myr) or, as above, it is much closer than 1 kpc in addition to being a binary.

### 5.3. *What is the relationship between the inner disk and the outer spiral?*

HV08 conjectured that the “reverse question mark”-shaped dark lane they observed in H $\alpha$  might be due to dust obscuration in front of the background nebula. We now see that the optical dark lane corresponds to the unilluminated region adjacent to the spiral nebula seen in our infrared data. Given the much greater penetrating power of 10-20  $\mu\text{m}$  radiation compared to visible light, producing the observed spiral pattern with a foreground dust cloud would require that cloud to both be very dense (to provide sufficient opacity at Q band) and have very sharply defined edges (so that the apparent spiral does not change in position or size with wavelength). That scenario is not impossible, but would require some fine-tuning of the dust cloud's properties. We may instead be looking at an actual physical structure rather than a line-of-sight superposition. In that case, it remains unclear what the spiral's origin might be.

Spiral density waves within circumstellar disks have now been observed around many YSOs (e.g. AB Aur, Grady et al. 1999; HD 141569, Clampin et al. 2003; HD 142527, Fukagawa et al. 2003), and are widely interpreted to be caused by the gravitational effects of orbiting companions. Since MWC 778 may well be a binary system, this seems at first to be an attractive explanation. But MWC 778's spiral differs from those seen around typical Herbig Ae/Be stars in several significant ways. First, it is much larger. Spiral structures, such as in the disks around AB Aur and HD 141569, are typically observed on a scale of 100-300 AU. In contrast, if MWC 778 truly is about 1 kpc distant, then the observed spiral is at least 12,000 AU across! Even more significantly, the spiral is not part of the circumstellar disk plane but instead appears to be oriented perpendicular to it. It is highly unlikely that a binary system whose orbital plane is aligned with the observed disk could produce a spiral with this orientation.

Instead of being part of the disk, the inner portions of the spiral apparently connect to MWC 778's polar axis, aligned with the bipolar cavities there. For some YSOs, precessing outflows have carved corkscrew-like bipolar cavities in their envelopes. Yet invoking outflows to carve the spiral around MWC 778 would require sufficient precession to turn the entire inner disk almost end-over-end in an impossibly short period of time ( $\sim 500$  years, for an observed size of 12000 AU and typical outflow velocities of 100 km/s). It is hard to see how this could be the case.

An alternate explanation for the spiral would be to invoke turbulence in molecular clouds, which is believed to create localized overdensities that can become unstable and collapse, leading to star formation. The curving nebula might then represent a residual filament of compressed material, which gave birth to the star but has not yet dispersed. A similar explanation

has been suggested for several binary YSOs which appear to be linked by bridges of material: e.g., LkH $\alpha$  225 (Perrin et al. 2004b) or SR 24 (Potter & Andrews 2002). Such a scenario would imply that the roughly symmetrical spiral appearance around MWC 778 is just a matter of chance.

## 6. CONCLUSIONS

Near-infrared polarimetric and mid-infrared imaging observations of the young stellar object MWC 778 have revealed a nearly-edge-on circumstellar disk plus bipolar outflow cavities, confirming the hypothesis advanced by HV08 on the basis of their spectra of the star and its nearby nebulosity. The images also reveal a large and intriguing spiral structure surrounding the star, prominent in all of the H $\alpha$ , near- and mid-infrared images. Because it appears to be oriented perpendicularly to the circumstellar disk plane, it is difficult to explain this as a spiral density wave similar to those seen in disks around many other young stars. The nature of this feature is currently unknown.

The presence of a disk suggests that previous values for the luminosity of the source may be underestimates; after correction for light blocked by the disk, the total bolometric luminosity at the assumed distance of 1 kpc now becomes at least  $\sim 750L_{\odot}$ . This leads to a paradox: that luminosity is far too large for the late-type spectral type derived by HV08 based on absorption features seen in the optical. Even the most luminous young F- and G-type stars, the intermediate mass T Tauri stars, are not expected to have luminosities in excess of  $\sim 100L_{\odot}$ .

We have suggested several possibilities to resolve this discrepancy: (1) the distance to MWC 778 may be vastly over-estimated, and it is really an IMTTS at a distance of a few hundred pc instead of 1 kpc; (2) the F-G-type absorption features may arise from the atmosphere of the circumstellar disk rather than the stellar photosphere, in which case the star itself becomes most plausibly a young Be star; (3) the system may actually be a binary composed of a B star and an F star. The currently available data do not allow us to determine which of these possibilities is correct, and in fact they are not mutually exclusive.

How might we test any of these hypotheses for the central source? The highest priority may be further spectroscopic observations, both to obtain increased temporal coverage in search of radial velocity variations from orbital motion, and to obtain higher signal-to-noise on the various absorption features to better constrain the apparent spectral type. Given the faintness of this source in the optical ( $V \sim 14$ ) such observations will be challenging. Further observations of the disk may provide indirect constraints on the stellar properties. Mapping the region in molecular emission lines (e.g. CO) could detect Keplerian rotation in the disk, providing kinematic constraints on the mass of the central object. Tighter constraints on the maximum amount of ionizing radiation present could potentially be obtained through flux-calibrated H $\alpha$  imaging—but such measurements would need to account for accretion luminosity and would be fraught with difficulties. Lastly, deeper wide-field imaging in the infrared should be obtained in order to search for additional nearby embedded sources that might be present; if any associated young but less deeply-

embedded sources can be found, their properties may provide complimentary constraints on the distance.

High contrast imaging observations are a powerful tool for investigating circumstellar environments and the physical processes at work therein, particularly when multiwavelength observations are available for analysis (e.g. Watson et al. 2007; Pinte et al. 2008). The spatially resolved observations presented here are a first step towards applying such a “pan-chromatic” approach to the study of MWC 778’s disk. But detailed investigations of disk structure are unlikely to be fruitful without a better understanding of the illuminating source and the distance to the system. As is so often said, establishing accurate distances remains one of the most challenging tasks in astronomy—yet doing just that is likely a necessary first step in conclusively establishing the nature of MWC 778.

WDV would like to thank George Herbig for calling his attention to this source and for numerous discussions regarding its nature, and also thanks Goeran Sandell for his insight regarding Herbig Ae/Be stars. MDP thanks John Monnier for useful discussions. These observations were made possible by the dedicated and hard working staffs of the Lick and Gemini Observatories, and in particular MDP is most grateful for expert assistance from Elinor Gates, R. Scott Fisher, and Kevin Volk.

The data presented here were obtained as part of a thesis project by MDP, who was supported at that time by a NASA Michelson Graduate Fellowship administered by JPL, and is now supported by a NSF Astronomy & Astrophysics Postdoctoral Fellowship. JRG & MDP were supported in part by the National Science Foundation Science and Technology Center for Adaptive Optics, managed by the University of California at Santa Cruz under cooperative agreement No. AST-9876783. This paper is based in part on observations obtained at the Gemini Observatory, which is operated by the Association of Universities for Research in Astronomy, Inc., under a cooperative agreement with the NSF on behalf of the Gemini partnership: the National Science Foundation (United States), the Science and Technology Facilities Council (United Kingdom), the National Research Council (Canada), CONICYT (Chile), the Australian Research Council (Australia), Ministério da Ciência e Tecnologia (Brazil) and SECYT (Argentina). The Gemini observing time was made available through a time trade arrangement between Gemini and the W. M. Keck Observatory, which is operated as a scientific partnership among the California Institute of Technology, the University of California and the National Aeronautics and Space Administration, and was made possible by the generous financial support of the W.M. Keck Foundation. The authors wish to recognize and acknowledge the very significant cultural role and reverence that the summit of Mauna Kea has always had within the indigenous Hawaiian community. We are most fortunate to have the opportunity to conduct observations from this mountain.

## REFERENCES

- Allen, D. 1974, MNRAS, 168, 1
- Andrews, S. M. & Williams, J. P. 2007, ApJ, 659, 705
- Apai, D., Pascucci, I., et al. 2004, A&A, 415, 671
- Blitz, L., Fich, M. & Stark, A. A. 1982, ApJS, 49, 183
- Boulard, M.-H., Caux, E., et al. 1995, A&A, 300, 276
- Calvet, N., Muzerolle, J., Briceno, C., Hernández, J., Hartmann, L., Saucedo, J. L., & Gordon, K. D. 2004, AJ, 128, 1294
- Chiang, E. I., Joungh, M. K., et al. 2001, ApJ, 547, 1077
- Clampin, M., Krist, J. E., et al. 2003, AJ 126, 385
- Cohen, M., Walker, R. G., et al. 1999, AJ, 117, 1864
- Fich, M. 1993, ApJS, 86, 475
- Fukagawa, M., Tamura, M., et al. ApJ, 2003
- García-Lario, P., Manchado, A., Pych, W., & Pottasch, S. R. 1997, A&AS, 126, 479
- Gavel, D. T., Gates, E. L., et al. 2003, Proc. SPIE Vol. 4839, 354
- Glasse, A. C., Atad-Ettingui, E. I., et al. Proc. SPIE Vol. 2871, 1997, 1197
- Grady, C., Woodgate, B. E., et al. 1999, ApJ
- Hartmann, L. & Kenyon, S. J. 1996, ARAA, 34, 207
- Herbig, G. H. & Vacca, W. D. 2008, AJ, 136, 1995
- Kamp, I. & Dullemond, C. P. 2004, ApJ, 615, 991
- Kohoutek, L. 1969, Bull. astr. Inst. Czech, 20, 307
- Kuhn, J. R., Potter, D., et al. 2001, ApJ, 553, L189
- Lamers, H. J. G. L. M., Zickgraf, F.-J., de Winter, D., Houziaux, L., & Zorec, J. 1998, A&A, 340, 117
- Lloyd, J. P., Liu, M. C., et al. In "Proc. SPIE Vol. 4008, p. 814-821, Optical and IR Telescope Instrumentation and Detectors, Masanori Iye; Alan F. Moorwood; Eds.", vol. 4008. 2000, 814-821
- Marston, A. P. & McCollum, B. 2008, A&A, 477, 193
- Merrill, P.W. & Burwell, C.G. 1949, ApJ, 110, 387
- Palla, F. 2005, Proceedings of the International Astronomical Union
- Palla, F. & Stahler, S. 1990, ApJ, 360, L47
- Perrin, M. D., Graham, J. R., Kalas, P., Lloyd, J. P., Max, C. E., Gavel, D. T., Pennington, D. M., & Gates, E. L. 2004a, Science, 303, 1345
- Perrin, M. D., Graham, J. R., et al. SPIE Advancements in Adaptive Optics. Edited by Domenico B. Calia, 5490, 2004b, 309
- Perrin, M. D. 2006, Ph. D. Thesis, Univ. of California
- Perrin, M. D., Graham, J. R., & Lloyd, J. P. 2008, PASP, 120, 555
- Persson, S. E., Murphy, D. C., et al. 1998, AJ, 116, 2475
- Pinte, C., Padgett, D. L., et al. A&A, 489, 2008, 633
- Potter, D. E. & Andrews, S. M. 2002, BAAS, 34, 1217
- Roberts, L. C., Jr., Perrin, M. D., et al. In D. Bonaccini Calia, B. L. Ellerbroek, & R. Ragazzoni, eds., "Advancements in Adaptive Optics. Edited by Domenico B. Calia, Brent L. Ellerbroek, and Roberto Ragazzoni. Proceedings of the SPIE, Volume 5490, pp. 504-515 (2004).", 2004, 504-515
- Suárez, O., García-Lario, P., Manchado, A., Manteiga, M., Ulla, A., & Pottasch, S. R. 2006, A&A, 458, 173.
- Siess, L., Dufour, E., et al. 2000, A&A, 358, 593
- Simon, M., Dutrey, A., et al. 2000, ApJ, 545, 1034
- Vieira, S. L. A., Corradi, W. J. B., Alencar, S. H. P., Mendes, L. T. S., Torres, C. A. O., Quast, G. R., Guimaraes, M. M., & Da Silva, L. 2003, AJ, 126, 2971
- Watson, A. M., Stapelfeldt, K. R., et al. 2007, In B. Reipurth, D. Jewitt, & K. Keil, eds., "Protostars and Planets V," 523-538
- Whitney, B. A., Clayton, G. C., Schulte-Ladbeck, R. E., Calvet, N., Hartmann, L., & Kenyon, S. J. 1993, ApJ, 417, 687
- Whitney, B. A., Wood, K., et al. ApJ, 591, 2003, 1049.
- Wouterloot, J. G. A. & Brand, J. 1989, A&AS, 80, 149
- Wouterloot, J. G. A., Brand, J., & Fiegle, K. 1993, A&AS, 98, 589